Adaptive Controller Design for a Linear Motor Control System

TIAN-HUA LIU, Senior Member, IEEE
YUNG-CHING LEE
YIH-HUA CHANG
National Taiwan University of Science and Technology

Three different adaptive controllers for a permanent magnet linear synchronous motor (PMLSM) position-control system are proposed. The proposed controllers include: a backstepping adaptive controller, a self-tuning adaptive controller, and a model reference adaptive controller. The detailed systematic controller design procedures are discussed. A PC-based position control system is implemented. Several experimental results including transient responses, load disturbance responses, and tracking responses of square-wave, sinusoidal-wave, and triangular-wave commands are discussed and compared. The proposed system has a good robustness performance even though the inertia of the system is increased to 10 times. The experimental results validate the theoretical analysis.

Manuscript received April 21, 2003; revised December 3, 2003; released for publication December 26, 2003.

IEEE Log No. T-AES/40/2/831380.

Refereeing of this contribution was handled by W. M. Polivka.

Authors' current addresses: T. H. Liu and Y-H. Chang, Dept. of Electrical Engineering, National Taiwan University of Science and Technology, 43 Keelung Road, Section 4, Taipei 106, Taiwan, E-mail: (Liu@mail.ntust.edu.tw); Y-C. Lee, Mustek, Hsinchu, Taiwan.

I. INTRODUCTION

Modern control systems, such as manufacturing equipment, transportation, and robots, usually require high-speed/high-accuracy linear motions. Generally speaking, these linear motions are traditionally implemented using rotary motors with mechanical transmission mechanisms such as reduction gears and lead screws. Such mechanical transmissions, however, not only seriously reduce linear motion speed and dynamic response, but also introduce backlash, large frictional and inertial loads [1]. Recently, more and more industrial products, such as: semiconductor manufacturing equipment, X-Y driving devices, robots, and artificial hearts require high-speed/high-accuracy motions. The linear motors, which do not use mechanical transmissions, show promise for widespread use in these high-speed/high-accuracy systems [2–4].

Without using the conventional gears or ball screws, the permanent magnet linear synchronous motor (PMLSM), however, is more easily affected by load disturbance, torque ripple, and parameter variations. As a result, the design of a controller and load disturbance compensator is very important in PMLSM drives. Many researchers have focused on this area. For example, some researchers have used different algorithms to estimate and compensate the external disturbance load of the PMLSM drive system [5–7]. In addition, several researchers have proposed different control algorithms for PMLSM drive systems to improve their performance [8–15]. For example, the linearization method has been successfully used for a PMLSM [8]. This method, however, requires accurate parameters of the PMLSM and complex control procedures. Recently, some researchers have used fuzzy rules or neural networks to control PMLSM drives. The idea is new and good. However, it requires on-line training or designer experience. In addition, the execution of the fuzzy rules requires a lot of selections and that of the neural networks a lot of computations [9–11]. Some researchers proposed robust controllers for PMLSM drives [12–13]. The robust controller design is based on the parameters and model of the PMLSM. In the real world, unfortunately, the measurement of the parameters of the PMLSM is very difficult. To solve the difficulty, adaptive controllers have been proposed for the PMLSM [14–15].

Adaptive control does not require the accurate parameters of the motor. As a result, it can be a feasible control algorithm for a PMLSM. Some papers using adaptive control for PMLSM drives have been published. For example, Tan et al. proposed a robust adaptive compensator to reduce the friction and force ripple of the PMLSM. The work presented here, however, focuses on friction and force ripple compensation but not on position-loop

or speed-loop controller design [14]. Xu and Yao proposed adaptive robust controller design for a PMLSM. This paper, however, only focuses on self-tuning algorithm [15]. Three different control algorithms, which include backstepping adaptive control, model reference adaptive control, and self-tuning adaptive control algorithms are discussed and compared. The experimental results show that the proposed system can track a step-input command, a square-wave command, a triangular time-varying position command, and a sinusoidal time-varying position command well. It has a good load disturbance rejection capability as well. To the authors' best knowledge, this is the first time that the three different adaptive control algorithms are studied and compared practically to the PMLSM control system. In addition, the design and implementation of backstepping adaptive control and model reference control to a PMLSM are also new ideas, and have not been presented in previously published papers.

II. MATHEMATICAL MODEL

The mathematical model of a permanent magnet synchronous motor can be described, in the two-axis d-q synchronously rotating frame, by the following differential equations [8]:

$$pi_d = \frac{1}{L_d}\left(v_d - R_s i_d + \frac{\pi}{\tau} v_e L_q i_q\right) \tag{1}$$

$$pi_q = \left(\frac{1}{L_q} v_q - R_s i_q - \frac{\pi}{\tau} v_e L_d i_d - \sqrt{\frac{3}{2}}\frac{\pi}{\tau}\lambda_{\max} v_e\right) \tag{2}$$

where p is the differential operator d/dt, i_d and i_q are the d-axis and q-axis currents, L_d and L_q are the d- and q-axis inductances, v_d and v_q are the d-axis and q-axis stator voltages, R_s is the stator resistance, τ is the pole pitch, v_e is the velocity, and $\lambda_{\max}$ is the maximum flux linkage due to permanent magnet in each phase. The electro-mechanical equation of the PMLSM is

$$F_e = \frac{\pi}{\tau}\left[(L_d - L_q) i_d i_q + \sqrt{\frac{3}{2}}\lambda_{\max} i_q\right]. \tag{3}$$

In this paper, the PMLSM is a surface-mounted PMLSM. As a result, L_d is equal to L_q. Then, (3) can be simplified as

$$F_e = \sqrt{\frac{3}{2}}\frac{\pi}{\tau}\lambda_{\max} i_q \tag{4}$$

$$= K_t i_q \tag{5}$$

where K_t is the torque constant of the motor. The dynamic mechanical speed-movement equation is

$$pv_m = \frac{1}{M}(F_e - Bv_m - F_L) \tag{6}$$

and

$$v_m = \frac{2}{P_o} v_e \tag{7}$$

where v_m is the mechanical speed, M is the mass, B is the friction coefficient, F_L is the external force, and P_o is the pole number of the motor. The dynamic mechanical position-movement equation is

$$py_m = v_m \tag{8}$$

where y_m is the mechanical position of the motor.

III. CONTROLLER DESIGN

The proportional-integral (PI) controller has been widely used in industry for a long time due to its simplicity and reliability. Unfortunately, using a fixed PI controller, it is difficult to obtain both a good transient response and a good load disturbance rejection capability. To solve the difficulty, an adaptive controller has been proposed. Several different types of adaptive controllers have been discussed [14–15]. Here, three different types of adaptive controller are used to control the linear motor. The details are discussed as follows.

A. Backstepping Adaptive Controller Design

By substituting (5) into (6), we can obtain

$$\begin{aligned}\frac{d}{dt}v_m &= \dot{v}_m \\ &= \frac{1}{M}(F_e - F_L - Bv_m) \\ &= \frac{1}{M}(K_t i_q - F_L - Bv_m) \\ &= A_1 i_q + A_2 F_L + A_3 v_m\end{aligned} \tag{9}$$

where $A_1 = K_t/M$, $A_2 = -1/M$ and $A_3 = -B/M$ are the parameters of the system. In the real world, the motor parameters cannot be precisely measured. In addition, these parameters are varied while the motor is saturated or its temperature is increased. As a result, the real parameters of the system include the nominal parameters and their variations [14]. Then, (9) can be rewritten as

$$\begin{aligned}\dot{v}_m &= A_1 i_q + A_2 F_L + A_3 v_m + \Delta A_1 i_q + \Delta A_2 F_L + \Delta A_3 v_m \\ &= A_1 i_q + (A_2 F_L + \Delta A_1 i_q + \Delta A_2 F_L + \Delta A_3 v_m) + A_3 v_m \\ &= A_1 i_q + d_1 + A_3 v_m\end{aligned} \tag{10}$$

where d_1 is the amount of the parameter variations and external load, and it can be expressed as

$$d_1 = A_2 F_L + \Delta A_1 i_q + \Delta A_2 F_L + \Delta A_3 v_m. \tag{11}$$

The position error, the difference between the position command and the real position, is expressed as

$$e_1 = y_m^* - y_m. \tag{12}$$

From (12), we can take the derivation of the position error and express the result as

$$\dot{e}_1 = \dot{y}_m^* - \dot{y}_m. \tag{13}$$

We define the velocity command of the PMLSM as

$$\begin{aligned} v_m^* &= \dot{y}_m^* + De_1 + F\int e_1 dt \\ &= \dot{y}_m^* + De_1 + Fx_1 \end{aligned} \tag{14}$$

where e_1 is the position error. D is the proportional controller gain, F is the integral gain, and x_1 is the integral result of e_1. By taking the differential of (14), we can obtain

$$\dot{v}_m^* = \ddot{y}_m^* + D\dot{e}_1 + Fe_1. \tag{15}$$

After that, we can define the speed error of the motor as

$$e_2 = v_m^* - v_m. \tag{16}$$

By taking the differential of (16) and substituting (15) and (10) into it, we can easily obtain

$$\dot{e}_2 = \ddot{y}_m^* + D\dot{e}_1 + Fe_1 - A_1 i_q - d_1 - A_3 v_m. \tag{17}$$

Combining (8), (13), and (16), we can derive

$$\begin{aligned} \dot{e}_1 &= \dot{y}_m^* - \dot{y}_m \\ &= \dot{y}_m^* - v_m \\ &= \dot{y}_m^* - v_m^* + e_2. \end{aligned} \tag{18}$$

By substituting (14) into (18), we can easily obtain

$$\dot{e}_1 = -De_1 - Fx_1 + e_2. \tag{19}$$

Then, we can define a Lyapunov function as

$$V = \frac{1}{2}e_1^2 + \frac{1}{2}e_2^2 + \frac{1}{2}\frac{1}{\gamma}\tilde{d}_1^2 + \frac{1}{2}Fx_1^2 \tag{20}$$

where V is the Lyapunov function, e_1 is the position error, e_2 is the speed error, γ is the positive weighting factor, and $\tilde{d}_1$ is the error between the real uncertainty and the estimated uncertainty. The estimated error $\tilde{d}_1$ is defined as

$$\tilde{d}_1 = d_1 - \hat{d}_1 \tag{21}$$

where $\hat{d}_1$ is the estimating value of the total uncertainty d_1.

From (20), we can obtain the derivation of the Lyapunov function as

$$\dot{V} = e_1\dot{e}_1 + e_2\dot{e}_2 + \frac{1}{\gamma}\tilde{d}_1\dot{\tilde{d}}_1 + Fx_1e_1. \tag{22}$$

By combining (17), (19), (21), and (22), we can obtain

$$\begin{aligned} \dot{V} = &-De_1^2 + e_2[(1+F)e_1 + D\dot{e}_1 + \ddot{y}_m^* - A_1 i_q - \hat{d}_1 - \tilde{d}_1 - A_3 v_m] \\ &- \frac{1}{\gamma}\tilde{d}_1\dot{\hat{d}}_1. \end{aligned} \tag{23}$$

In this work, to simply the control algorithm, we assume the real current can track the current command well. Then, we set the current command as the control input, and it is expressed as

$$\begin{aligned} u = i_q^* &= i_q \\ &= \frac{1}{A_1}[(1+F)e_1 + D\dot{e}_1 + \ddot{y}_m^* - \hat{d}_1 - A_3 v_m + Ge_2] \end{aligned} \tag{24}$$

where i_q^* is the current command amplitude, and G is a positive gain.

Substituting (24) into (23), it is not difficult to obtain

$$\dot{V} = -De_1^2 - Ge_2^2 - \frac{1}{\gamma}\tilde{d}_1\dot{\hat{d}}_1 - \tilde{d}_1 e_2. \tag{25}$$

By designing an adaptive law $\dot{\hat{d}}_1 = -\gamma e_2$, we can remove the last two terms. Equation (25), therefore, can be reduced as

$$\dot{V} = -De_1^2 - Ge_2^2 \le 0. \tag{26}$$

In order to discuss the convergence of the drive system, the Barbalat's lemma is applied here. First, the function $Z(t)$ is defined as follows

$$Z(t) = -De_1^2 - Ge_2^2. \tag{27}$$

By integrating both sides of (27), we can obtain

$$\begin{aligned} \int_0^\infty Z(\tau)d\tau = &V(e_1(0), e_2(0), \tilde{d}_1(0)) \\ &- V(e_1(\infty), e_2(\infty), \tilde{d}_1(\infty)). \end{aligned} \tag{28}$$

The values of $e_1(0)$, $e_2(0)$, and $\tilde{d}_1(0)$ are bounded. In addition, the $\dot{V} \le 0$, therefore, the values of $e_1(\infty)$, $e_2(\infty)$, and $\tilde{d}_1(\infty)$ are also bounded. Then, from (28), we can observe that the integration of $Z(t)$ is bounded. From (27), it is easy to understand that the integration of the position error square $e_1^2(t)$ and the integration of the speed error square $e_2^2(t)$ are bounded as well. After deriving that the $e_1(t)^2$ and $e_2(t)^2$ are uniformly continuous, one can use Barbalat's lemma and obtain that

$$\lim_{t\to\infty} Z(t) = 0. \tag{29}$$

Equation (29) means while the time approaches infinite, the position error and the speed error converge to zero. As a result, the proposed PMLSM

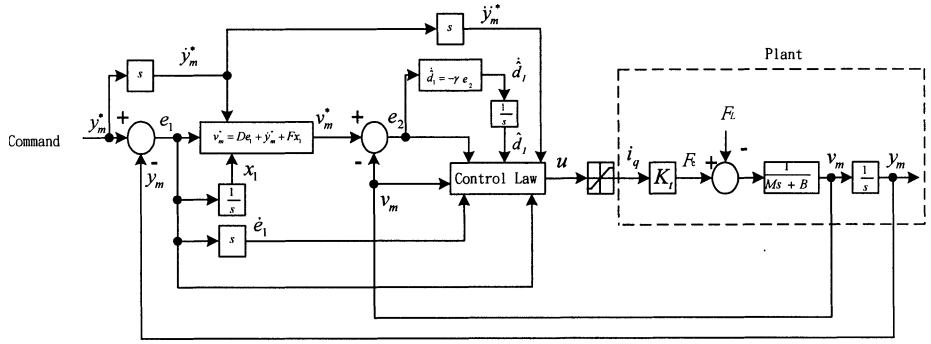

Fig. 1. Block diagram of backstepping adaptive control system.

drive system is stable. The block diagram of the proposed closed-loop drive system is shown in Fig. 1.

B. Self-Tuning Adaptive Controller Design

Equation (9) can be easily rewritten as

$$\bar{M}\dot{v}_m = -\bar{B}v_m + i_q - \bar{F}_L. \tag{30}$$

The parameters of (30) can be defined as follows

$$\bar{M} = \frac{M}{K_t} \tag{30a}$$

$$\bar{B} = \frac{B}{K_t} \tag{30b}$$

$$\bar{F}_L = \frac{F_L}{K_t}. \tag{30c}$$

Then, by substituting (8) into (30), we can obtain

$$\bar{M}\ddot{y}_m = -\bar{B}\dot{y}_m + i_q - \bar{F}_L. \tag{31}$$

In this work, we select the variable W as

$$W = \lambda_1 e_1 + e_2 = \lambda_1 e_1 + \dot{e}_1. \tag{32}$$

By taking the differential of (32), we can obtain

$$\dot{W} = \lambda_1 \dot{e}_1 + \dot{e}_2. \tag{33}$$

Then, by combining (13), (16), (31), and (33), we can obtain

$$\begin{aligned}\bar{M}\dot{W} &= \bar{M}[\lambda_1(\dot{y}_m^* - \dot{y}_m) + (\dot{v}_m^* - \dot{v}_m)] \\ &= -i_q + \bar{M}(\lambda_1 e_2 + \dot{v}_m^*) + \bar{B}v_m + \bar{F}_L.\end{aligned} \tag{34}$$

In the real world, however, the $\bar{M}$, $\bar{B}$, and $\bar{F}_L$ cannot be precisely measured. The estimated parameters to replace the real parameters of the motor are used here. We select the estimating parameter vector as

$$\hat{\theta}^T = [\hat{\bar{M}} \quad \hat{\bar{B}} \quad \hat{\bar{F}}_L]. \tag{35}$$

Then, we define the state vector $\bar{Y}$ as

$$\bar{Y} = [\lambda_1 e_2 + \dot{v}_m^* \quad v_m \quad 1]^T. \tag{36}$$

By substituting (35) and (36) into (34), we can obtain

$$\bar{M}\dot{W} = -i_q + \theta^T \bar{Y}. \tag{37}$$

We select the control input i_q as

$$i_q = \hat{\theta}^T \bar{Y} + \lambda_2 W \tag{38}$$

substituting (38) into (37), it is not difficult to obtain

$$\bar{M}\dot{W} = \phi^T \bar{Y} - \lambda_2 W \tag{39}$$

and

$$\begin{aligned}\phi^T &= \theta^T - \hat{\theta}^T \\ &= [\bar{M} - \hat{\bar{M}} \quad \bar{B} - \hat{\bar{B}} \quad \bar{F}_L - \hat{\bar{F}}_L].\end{aligned} \tag{40}$$

We select the Lyapunov function V as [16]

$$V = \tfrac{1}{2}\gamma_1 \bar{M} W^2 + \tfrac{1}{2}\phi^T \phi. \tag{41}$$

By taking the differential of equation (41), we can obtain

$$\dot{V} = \gamma_1 W \bar{M}\dot{W} + \phi^T \dot{\phi}. \tag{42}$$

Substituting (39) into (42), we can obtain

$$\dot{V} = \phi^T(\gamma_1 W \bar{Y} + \dot{\phi}) - \gamma_1 \lambda_2 W^2. \tag{43}$$

We select the adaptive law as

$$\dot{\phi} = -\gamma_1 W \bar{Y}. \tag{44}$$

Substituting (44) into (43), we can obtain

$$\dot{V} = -\gamma_1 \lambda_2 W^2. \tag{45}$$

From (39), we can derive

$$\begin{aligned}\int_0^\infty W^2 d\tau &= -\frac{1}{\gamma_1 \lambda_2}\int_0^\infty \dot{V} d\tau \\ &= \frac{1}{\gamma_1 \lambda_2}[V(0) - V(\infty)].\end{aligned} \tag{46}$$

The W is bounded because $V(0)$ and $V(\infty)$ are bounded. In addition, the W is uniformly continuous. According to Barbalat's lemma, we can obtain

$$\lim_{t\to\infty} W(t) = 0. \tag{47}$$

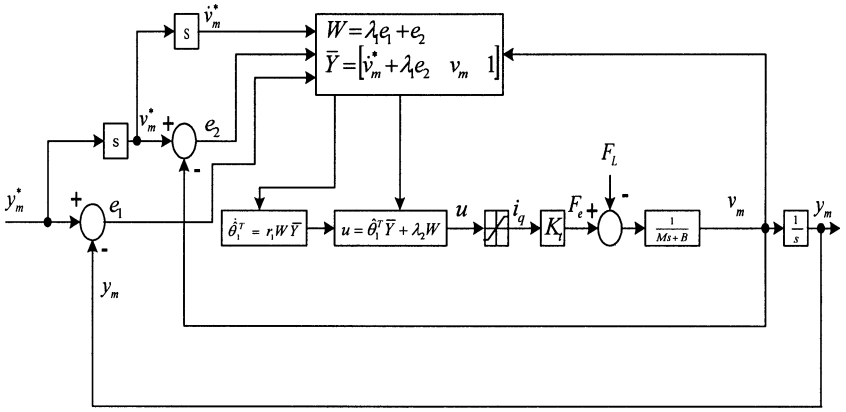

Fig. 2. Block diagram of self-tuning control system.

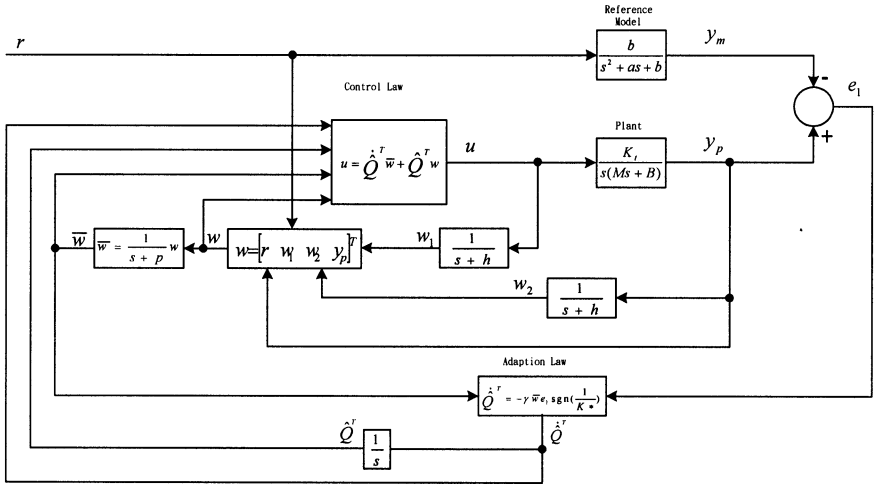

Fig. 3. Block diagram of model reference control system.

Then, from (32), we can obtain

$$\lim_{t\to\infty} e_1(t) = 0. \tag{48}$$

Equation (48) shows that using a self-tuning controller and in steady-state condition, the position error of the PMLSM is equal to zero. The block diagram of the self-tuning control system is shown in Fig. 2.

C. Model Reference Adaptive Controller Design

The proposed model reference adaptive PMLSM position control system is shown in Fig. 3. By on-line adjusting the feedback gains, the PMLSM position control system can match the reference model well. The details are discussed as follows.

In order to obtain a model reference adaptive controller, an adaption law is used here to adjust the feedback gain vector to an ideal vector Q^*. First, define the control input u as

$$u = Q^* w = [K \quad Q_1^* \quad Q_2^* \quad Q_3^*] \begin{bmatrix} r \\ w_1 \\ w_2 \\ y_p \end{bmatrix} \tag{49}$$

where Q^* is the ideal feedback gain vector . According to Fig. 3, the dynamic system can be described as

$$\begin{aligned} \dot{Y}_c &= \begin{bmatrix} A_p & 0 & 0 \\ 0 & -h & 0 \\ C_p^T & 0 & -h \end{bmatrix} \begin{bmatrix} x_p \\ w_1 \\ w_2 \end{bmatrix} + \begin{bmatrix} B_p \\ 1 \\ 0 \end{bmatrix} u \\ &= A_{c1} Y_c + B_c u. \end{aligned} \tag{50}$$

In (50), it is easy to observe that

$$A_{c1} = \begin{bmatrix} A_p & 0 & 0 \\ 0 & -h & 0 \\ C_p^T & 0 & -h \end{bmatrix} \tag{51}$$

and

$$B_c = \begin{bmatrix} B_p \\ 1 \\ 0 \end{bmatrix}, \qquad Y_c = \begin{bmatrix} x_p \\ w_1 \\ w_2 \end{bmatrix}. \tag{52}$$

Equation (50) includes two parts: the uncontrolled system states x_p and the feedback controller states w_1 and w_2. The uncontrolled system dynamics can

be described as

$$\begin{aligned}\dot{x}_p &= \begin{bmatrix}\dot{y}_r \\ \dot{v}_r\end{bmatrix} \\ &= \begin{bmatrix}0 & 1 \\ 0 & \dfrac{-B}{M}\end{bmatrix}\begin{bmatrix}y_r \\ v_r\end{bmatrix} + \begin{bmatrix}0 \\ \dfrac{K_t}{M}\end{bmatrix} u \\ &= A_p x_p + B_p u \end{aligned} \tag{52a}$$

and

$$\begin{aligned} y_p &= C_p^T x_p \\ &= [1 \quad 0]\begin{bmatrix}y_r \\ v_r\end{bmatrix}. \end{aligned} \tag{52b}$$

Next, we derive the closed-loop system dynamic equation. First, by substituting control u shown in (49) into (50), and suitably arrange it, we can obtain

$$\begin{aligned}\dot{Y}_c &= A_{c1}Y_c + B_c u \\ &= A_{c1}Y_c + B_c Q^{*T} w + B_c(u - Q^{*T} w) \\ &= A_c Y_c + B_c K^{*T} r + B_c(u - Q^{*T} w) \end{aligned} \tag{53a}$$

and

$$\begin{aligned} y_p &= C_P^T x_p \\ &= [C_p^T 00] Y_c \\ &= C_c^T Y_c. \end{aligned} \tag{53b}$$

In (53a), the matrix A_c is expressed as

$$A_c = \begin{bmatrix} A_p + B_p Q_3^* C_p^T & B_p Q_1^* & B_p Q_2^* \\ Q_3^* C_p^T & -h + Q_1^* & Q_2^* \\ C_p^T & 0 & -h \end{bmatrix}. \tag{54}$$

In this paper, the reference model is expressed as

$$\dot{Y}_m = A_c Y_m + B_c K^* r \tag{55}$$

and

$$y_m = C_c^T Y_m \tag{56}$$

where Y_m is the output vector, and y_m is the position of the motor.

From (53a) and (55), we can obtain

$$\begin{aligned}\dot{e} &= \dot{Y}_c - \dot{Y}_m \\ &= A_c e + B_c(u - Q^{*T} w) \end{aligned} \tag{57}$$

and

$$e_1 = C_c^T e \tag{58}$$

where e is the error vector between the real output vector Y_c and the reference output vector Y_m, and e_1 is the error between the real position y_p and the reference position y_m. According to (55)–(56), we can obtain

$$\begin{aligned} y_m &= C_c^T (sI - A_c)^{-1} B_c K^* r \\ &= W_m(s) r. \end{aligned} \tag{59}$$

In (59), we can observe that the transfer function of the model reference is

$$W_m(s) = C_c^T (sI - A_c)^{-1} B_c K^*. \tag{60}$$

Substituting (60) into (57) and (58), we can derive

$$e_1 = \frac{1}{K^*} W_m(s)(u - Q^{*T} w). \tag{61}$$

In order to make the adaptive control system track a second-order reference model, the error dynamic can be modified as follows:

$$\begin{aligned}\dot{e} &= A_c e + B_c K^* \frac{1}{K^*}(u - Q^{*T} w)(s+p)(s+p)^{-1} \\ &= A_c e + B_{c1} \frac{1}{K^*}(u_1 - Q^{*T} \bar{w})(s+p). \end{aligned} \tag{62}$$

From (62), we can observe that

$$B_{c1} = B_c K^* \tag{63}$$

$$u_1 = (s+p)^{-1} u \tag{64}$$

$$\bar{w} = (s+p)^{-1} w. \tag{65}$$

In the real world, Q^* is unknown. As a result, the control input is selected as

$$u = \hat{Q}^T w. \tag{66}$$

Then, from (64)–(66), we can observe

$$u_1 = \hat{Q}^T \bar{w}. \tag{67}$$

By substituting (67) into (62), we can derive that the error dynamic equations are expressed as

$$\dot{e} = A_c e + B_{c1} \frac{1}{K^*} \tilde{Q}^T \bar{w}(s+p). \tag{68}$$

In addition, by substituting (65) and (66) into (61), we can derive

$$e_1 = \frac{1}{K^*} W_m(s) \tilde{Q}^T \bar{w}(s+p) \tag{69}$$

where $\tilde{Q}^T$ is the error between $\hat{Q}^T$ and Q^{*T}.

By comparing (64) and (67), we can obtain

$$\begin{aligned} u &= (s+p)u_1 \\ &= (s+p)\hat{Q}^T \bar{w} \\ &= \dot{\hat{Q}}^T \bar{w} + \hat{Q}^T w. \end{aligned} \tag{70}$$

The parameter $\dot{\hat{Q}}^T$ is obtained from adaptation law. In order to derive the adaptation law, selecting a suitable Lyapunov function is required. To define a Lyapunov function, a new parameter $\bar{e}$ is defined as

$$\bar{e} = e - B_{c1} \frac{1}{K^*} \tilde{Q}^T \bar{w}. \tag{71}$$

Taking the differential value of (71) and substituting it into (68), we can obtain

$$\dot{\bar{e}} = A_c \bar{e} + (A_c B_{c1} + B_{c1} p) \frac{1}{K^*} \tilde{Q}^T \bar{w}. \tag{72}$$

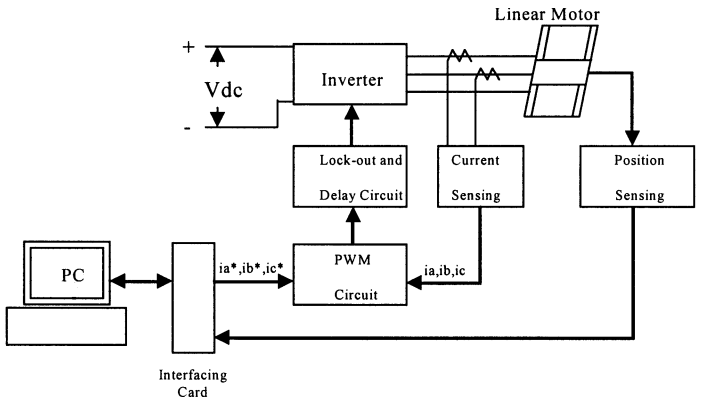

Fig. 4. Implemented system.

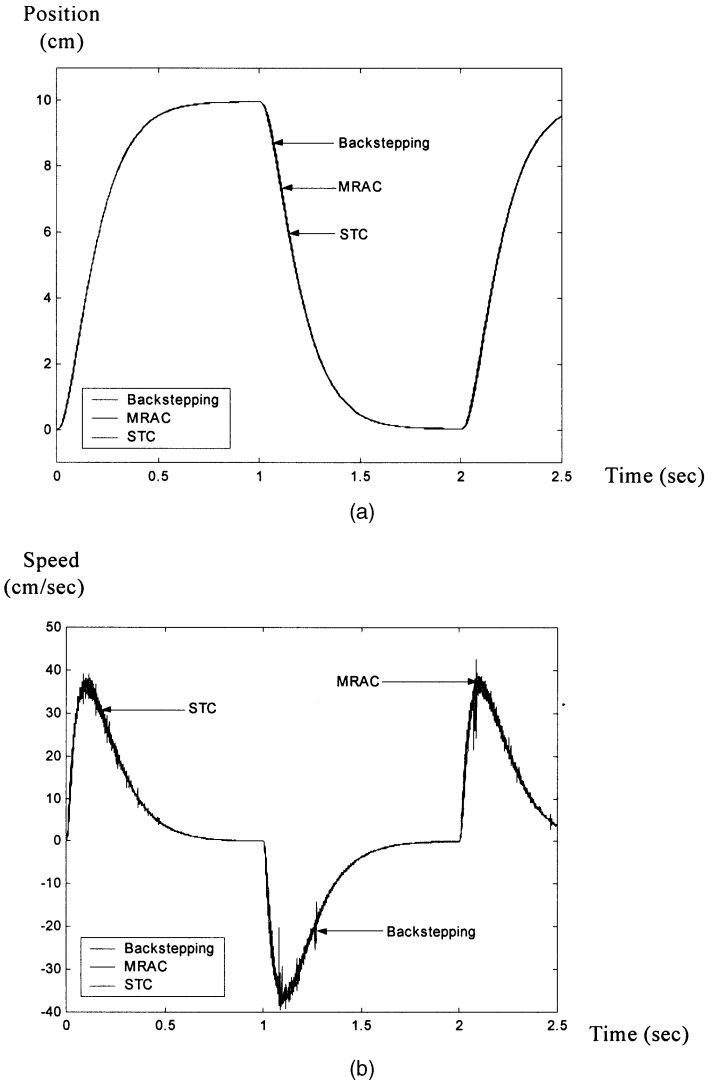

Fig. 5. Measured square-wave position responses for thee different controllers. (a) Position (b) Speed.

Rearranging (71) and substituting it into (58), we can obtain

$$e_1 = C_c^T \bar{e}. \tag{73}$$

Next, we select a Lyapunov function

$$V = \bar{e}^T P_c \bar{e} + \frac{1}{2}\tilde{Q}^T \gamma^{-1} \tilde{Q} \left| \frac{1}{K^*} \right| \tag{74}$$

and P_c satisfies the following two equations:

$$A_c^T P_c + P_c A_c = -Q \tag{75}$$

and

$$P_c B_{c1} = C_c. \tag{76}$$

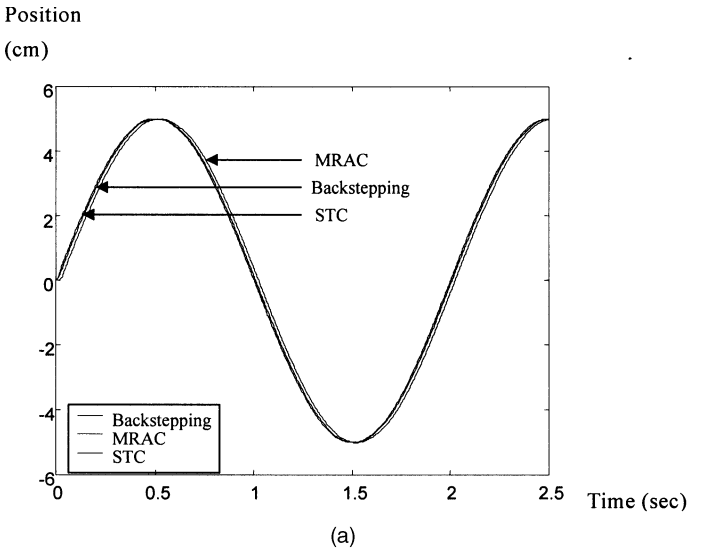

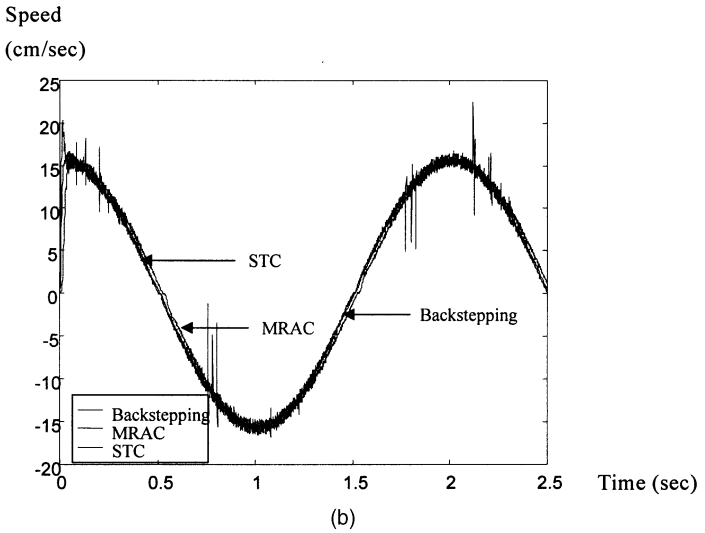

Fig. 6. Measured sinusoidal-wave responses. (a) Position. (b) Speed.

Taking the derivative of (74), and substituting (75)–(76) into the derivative result, we can obtain

$$\dot{V} = -\bar{e}^T Q \bar{e} + \tilde{Q}^T \left(e_1 \frac{1}{K^*} \bar{w} + \gamma^{-1} \dot{\hat{Q}} \left| \frac{1}{K^*} \right| \right). \quad (77)$$

In this paper, finally, we choose the adaption law as

$$\dot{\hat{Q}} = -\gamma \bar{w} e_1 \operatorname{sgn}\left(\frac{1}{K^*} \right). \quad (78)$$

In (78), we define

$$\operatorname{sgn}\left(\frac{1}{K^*} \right) = \frac{|K^*|}{K^*}. \quad (79)$$

Substituting (78) into (77), we can obtain

$$\dot{V} = -\bar{e}^T Q \bar{e} \leq 0. \quad (80)$$

Equation (80) shows that the $\bar{e}$ is a nonincreasing variable. The proposed system, therefore, is a stable position-control system.

IV. IMPLEMENTATION

The implemented system is shown in Fig. 4. The control system includes four major parts: the linear motor, the inverter, the personal computer, and the sensing and pulsewidth modulation (PWM) circuits. The personal computer is used to execute the control algorithms. The feedback signals and the control inputs are connected between the hardware circuits and the personal computer through the interfacing card. The sensing circuits include the position sensing circuit and the current sensing circuit. The PWM signals are obtained by using a 5 kHz triangular waveform to modulate the three-phase current deviations. The lock-out circuit and the delay circuit are implemented to avoid the short-circuit between the upper leg and lower leg of the inverter. The three-phase linear motor is driven by the inverter, which is implemented by using six insulated gate bipolar transistors (IGBTs). The input voltage of the inverter is around 154 V dc voltage, which is

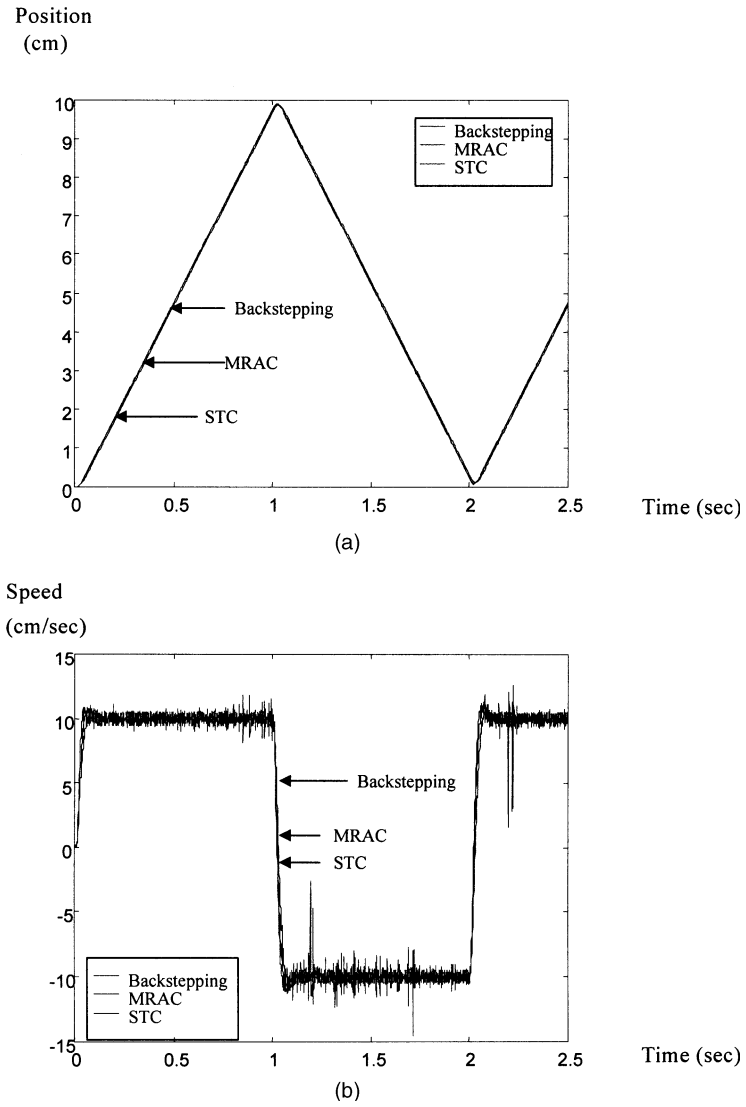

Fig. 7. Measured triangular-wave responses. (a) Position. (b) Speed.

obtained from an ac 110 V with a full-wave rectifier and a 1000 μF filtering capacitance. As a result, the input voltage of the inverter is a smooth dc voltage source. The motor is a 3-phase, 4-pole PMLSM. The parameters of the motor are: R_s = 1.05 Ω, $L_d = L_q$ = 0.4 mH, K_t = 14.3 Nt/A, M = 1.8 Kg, and B = 5 Nt.s/m. After suitable feedback of the current and position sensing signals of the linear motor, the three-phase currents of the linear motor can be adjusted. As a result, a closed-loop control system is achieved.

V. EXPERIMENTAL RESULTS

In this paper, the linear permanent magnet synchronous motor was made by Kollmorgen Company, typed IL 6-050. The accuracy of the position sensor is 1 μm. The current limit of the proposed system is ±10 A. The sampling interval of the position control is 1 ms. Some measured waveforms are provided here to validate the theoretical analysis. Fig. 5(a)–(b) show the measured square-wave position responses for three different controllers. Fig. 5(a) is the measured position response and Fig. 5(b) is the relative speed response. As you can observe, the three different controllers have similar responses. Fig. 6(a)–(b) show the measured sinusoidal-wave command responses. Fig. 6(a) is the position response. Fig. 6(b) is the relative speed response. The three different controllers perform different phase-lags; however, they are very close. Fig. 7(a)–(b) show the measured triangular-wave position responses. Fig. 7(a) shows the position responses and Fig. 7(b) shows the relative speed responses. Again, the three different controllers have similar position and speed responses. In Fig. 6(b) and Fig. 7(b), there are several spikes. The major reason is that the speed signal is the derivation of the position signal. As a result, a small noise in position signal can generate a large spike in the speed

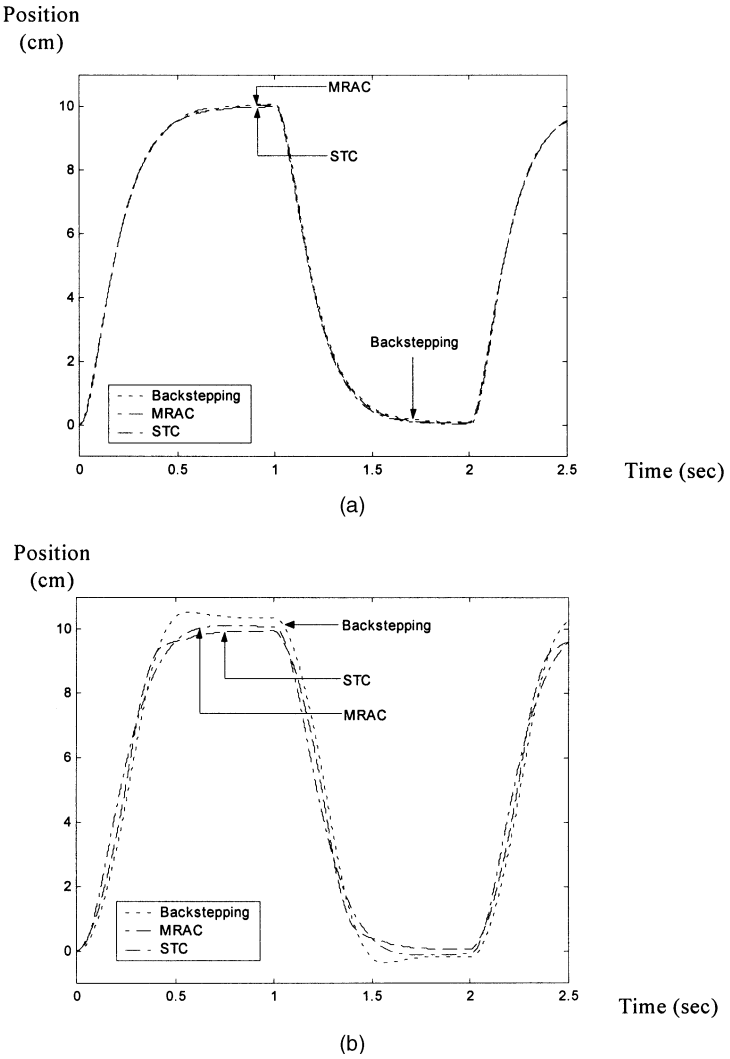

Fig. 8. Measured square-wave position responses. (a) With a 20 Nt load. (b) With a 10 times inertia.

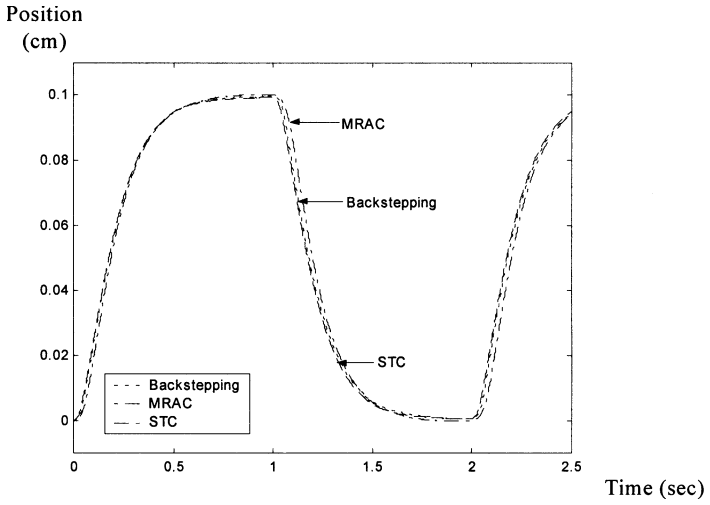

Fig. 9. Measured short-distance position responses.

signal. Fig. 8(a) shows the measured square-wave position response under an external load of 20 Nt. The proposed controllers have good load disturbance rejection capability. Fig. 8(b) shows the measured square-wave position response when the inertia of the system in increased to 10 times. According to the

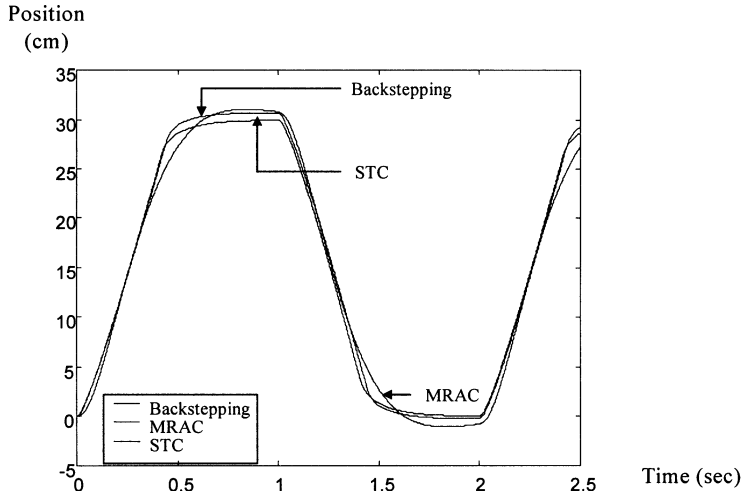

Fig. 10. Measured long-distance position responses.

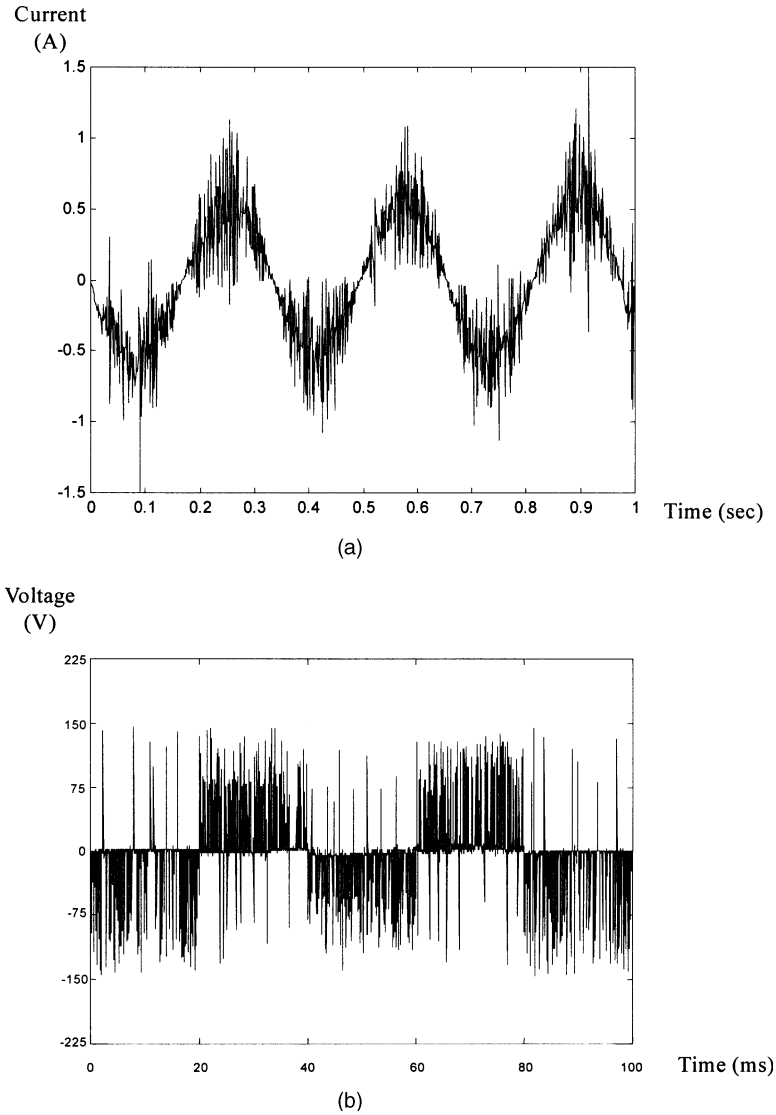

Fig. 11. Steady-state waveforms of a triangular position command. (a) Current. (b) Voltage.

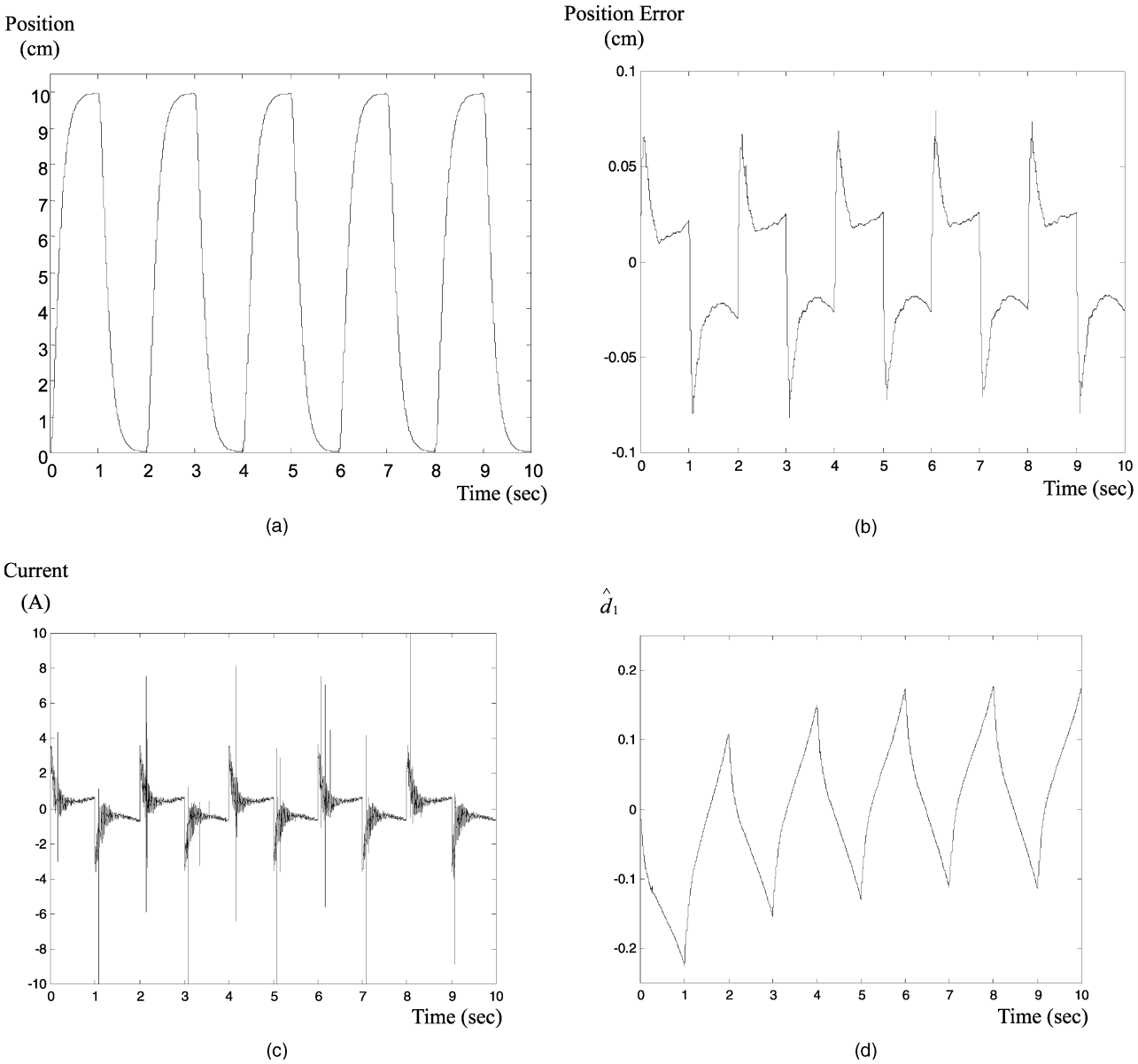

Fig. 12. Waveforms of square-wave command using backstepping adaptive controller. (a) Position. (b) Position error. (c) q-axis current. (d) Uncertainty $\hat{d}_1$.

experimental results, the differences of the position responses are more obvious when the inertia of the system is varied. In addition, the self-tuning adaptive controller and the model reference adaptive controller perform better than the backstepping adaptive controller. Fig. 9 shows the measured short-distance position responses at a 0.1 cm movement. Fig. 10 shows the measured long-distance position responses at a 30 cm movement. Figs. 11(a)–(b) show the measured steady-state current and voltage waveforms of a triangular position command. Fig. 11(a) is the measured a-phase current; Fig. 11(b) is the measured line-to-line voltage between the a-phase and b-phase. The measured current is near a sinusoidal waveform and the line-to-line voltage amplitude is around 150 V. Figs. 12(a)–(d) show the measured waveforms of a square-wave command using the proposed backstepping adaptive controller. Fig. 12(a) is the measured position response of a square-wave command. Fig. 12(b) is the relative position error. Fig. 12(c) is the measured q-axis current. Fig. 12(d) is the estimated uncertainty $\hat{d}_1$. Figs. 13(a)–(d) show the measured waveforms of a square-wave command by using a model reference controller. Fig. 13(a) is the position response; Fig. 13(b) is the position error response. Fig. 13(c) is the q-axis current response. Some parameters of the model reference controller are also measured. Fig. 13(d) is the measured parameter of $\hat{K}^*$. Fig. 13(e)–(g) show the measured parameters of $\hat{Q}_3^*$, $\hat{Q}_2^*$, and $\hat{Q}_1^*$ respectively. As you can see, the parameters converge to near constant values as time increases. According to the experimental results,

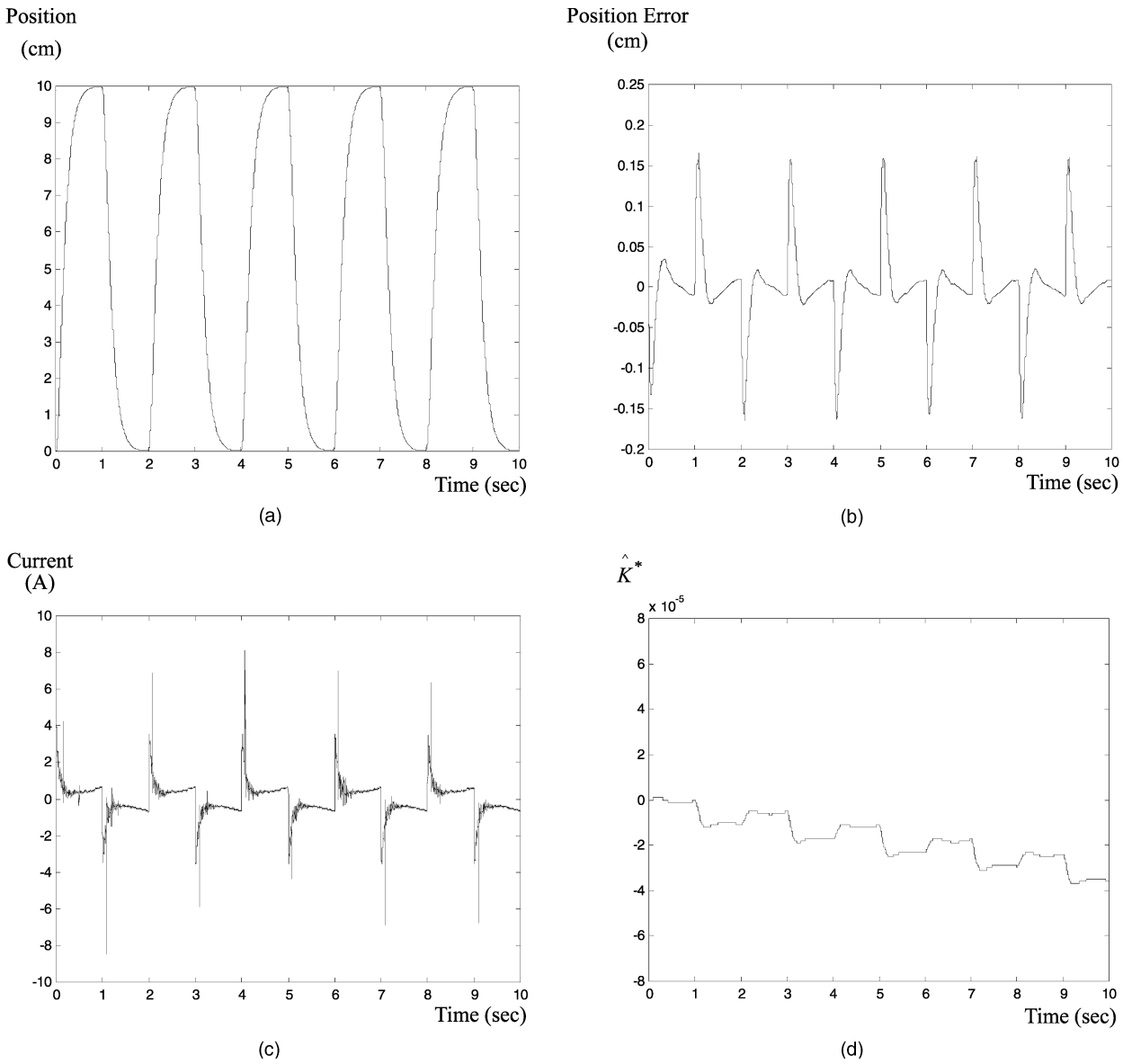

Fig. 13. Square-wave position responses using model reference controller. (a) Position. (b) Position error. (c) q-axis current. (d) Parameter $\hat{K}^*$.

the three different controllers have a very similar steady-state position error, which is ± 1 μm. For a linear motor drive, both steady-state performance and transient response are important. In order to evaluate the dynamic performance, the different performance indices, which are the integration of the square of the position error, are shown in Table I. The unit of Table I is cm^2.s. As you can observe, the three controllers have different performance indices. For the time-varying sinusoidal-wave command, the triangular-wave command, and the inertia varying case, the model reference adaptive controller performs better than the other controllers. On the other hand, for square-wave command, the self-tuning adaptive controller has the best performance. Generally speaking, the backstepping adaptive controller has the simplest computing process; however, its performance is a little worse as compared with the two other controllers. According to the results of Table I, the designer can select different adaptive controller to satisfy their real applications. For example, if the applications focus on triangular-command position control, the model reference adaptive controller is the best choice. On the other hand, if the applications focus on square-wave control or step-input control, the self-tuning adaptive controller is the best candidate. The detailed design procedures of the controllers are clearly discussed and proved here. In the real world, there are some difficulties that should be faced. The selection of the tuning parameters relies on the designer's experience. For example, the designer should properly choose the following parameters: D, F, G, and γ of the backstepping adaptive controller, λ_1, λ_2, and γ_1 of the self-tuning controller, and p, h,

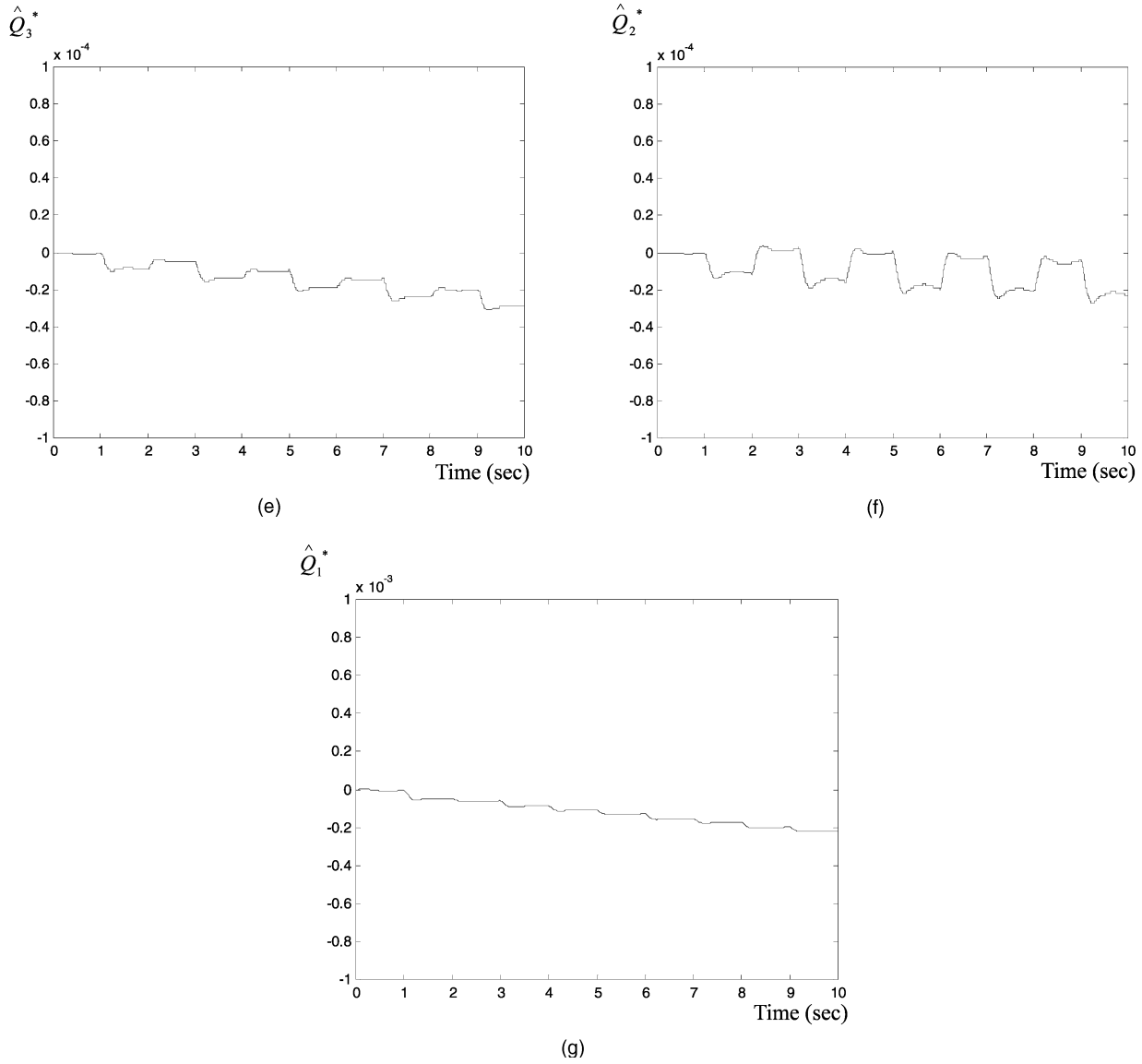

Fig. 13. *Continued.* (e) Parameter $\hat{Q}_3^*$. (f) Parameter $\hat{Q}_2^*$. (g) Parameter $\hat{Q}_1^*$.

TABLE I
Integration of Square of Position Error for Different Controllers

Command	Controller Backstepping	STC	MRAC
square 10 cm	0.003801	0.001097	0.004646
sinusoidal 5 cm	0.000934	0.000785	0.000028
triangular 10 cm	0.000442	0.000624	0.000042
square 10 cm and 20 Nt	0.018698	0.002218	0.011230
square 10 cm and 10 times inertia	2.975864	1.616673	0.870155
square 0.1 cm	0.0000036	0.00000072	0.000026
square 30 cm	21.876602	22.876022	25.184871

γ of the model reference controller. As a result, doing computer simulation is required before executing the implementation. By using this way, a lot time in trial and error can be reduced.

VII. CONCLUSIONS

In this paper, three different adaptive control techniques have been applied to a PMLSM. The systematic design procedures have been discussed. By using the proposed controllers, the PMLSM control system has satisfactory performance in transient response, load disturbance rejection capability, and tracking ability. Several varying commands are used to evaluate the proposed PMLSM system. This paper proposes three design methods of the adaptive controller for a PMLSM position control system.

REFERENCES

[1] Otten, G., Vries, J. A., Amerongen, J. V., Rankers, A. M., and Gaal, E. W. (1997)
Linear motor motion control using a learning feedforward controller.
IEEE/ASME Transactions on Mechatronics, **2**, 3 (Sept. 1997), 179–187.

[2] Yoshida, K., Takami, H., Kong, X., and Sonoda, A. (2001)
Mass reduction and propulsion control for a permanent-magnet linear synchronous motor vehicle.
IEEE Transactions on Industry Applications, **37**, 1 (Jan./Feb. 2001), 67–72.

[3] Lorenz, R. D., Zik, J. J., and D. J. (1991)
A direct-drive, robot parts, and tooling gripper with high-performance force feedback control.
IEEE Transactions on Industry Applications, **27**, 2 (Mar./Apr. 1991), 275–281.

[4] Yamada, H., Nirei, M., Kawakatu, K., Yamamoto, Y., and Miwa, Z. (1987)
Characteristics of assist device for artificial heart using linear pulse motor.
IEEE Transactions on Magnetics, **23**, 5 (Sept. 1987), 3011–3013.

[5] Egami, T., and Tsuchiya, T. (1995)
Disturbance suppression control with preview action of linear dc brushless motor.
IEEE Transactions on Industrial Electronics, **42**, 5 (Oct. 1995), 494–500.

[6] Kempf, C. J., and Kobayashi, S. (1999)
Disturbance observer and feedforward design for a high-speed direct-drive positioning table.
IEEE Transactions on Control System Technology, **7**, 5 (Sept. 1999), 513–526.

[7] Komada, S., Ishida, M., Ohnishi, K., and Hori, T. (1991)
Disturbance observer-based motion control of direct drive motors.
IEEE Transactions on Energy Conversion, **6**, 3 (Sept. 1991), 553–559.

[8] Famouri, P. (1992)
Control of a linear permanent magnet brushless dc motor via exact linearization methods.
IEEE Transactions on Energy Conversion, **7**, 3 (Sept. 1992), 544–551.

[9] Lin, F. J., Wai, R. J., and Hong, C. M. (2001)
Hybrid supervisory control using recurrent fuzzy neural network for tracking periodic inputs.
IEEE Transactions on Neural Networks, **12**, 1 (Jan. 2001), 68–90.

[10] Tan, K. K., Dou, H., Chen, Y., and Lee, T. H. (2001)
High precision linear motor control via relay-tuning and iterative learning based on zero-phase filtering.
IEEE Transactions on Control Systems Technology, **9**, 2 (Mar. 2001), 244–253.

[11] Vries, T. J. A., Velthuis, W. J. R., and Idema, L. J. (2001)
Application of parsimonious learning feedforward control to mechatronic systems.
IEE Proceedings—Control Theory Applications, **148**, 4 (July 2001), 318–322.

[12] Shieh, N. C., and Tung, P. C. (2001)
Robust output tracking control of a linear dc brushless motor for transportation in manufacturing system.
IEE Proceedings—Electric Power Applications, **148**, 2 (Mar. 2001), 119–124.

[13] Liaw, C. M., Shue, R. Y., Chen, H. C., and Chen, S. C. (2001)
Development of a linear brushless dc motor drive with robust position control.
IEE Proceedings—Electric Power Applications, **148**, 2 (Mar. 2001), 111–118.

[14] Tan, K. K., Huang, S. N., and Lee, T. H. (2002)
Robust adaptive numerical compensation for friction and force ripple in permanent-magnet linear motors.
IEEE Transactions on Magnetics, **38**, 1 (Jan. 2002), 221–228.

[15] Xu, L., and Yao, B. (2001)
Adaptive robust precision motion control of linear motors with negligible electrical dynamics: Theory and experiments.
IEEE/ASME Transactions on Mechatronics, **6**, 4 (Dec. 2001), 444–452.

[16] Wang, W. J., and Wang, C. C. (1998)
A new composite adaptive speed controller for induction motor based on feedback linearization.
IEEE Transactions on Energy Conversion, **13**, 1 (Mar. 1998), 1–6.

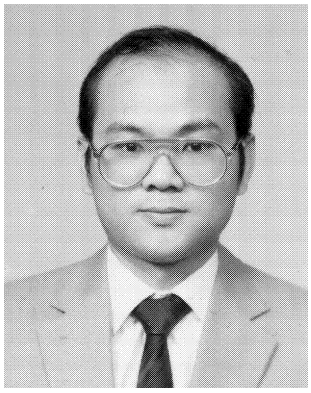

Tian-Hua Liu (S'85—M'89—SM'99) was born in Tao Yuan, Taiwan, Republic of China, on November 26, 1953. He received the B.S., M.S., and Ph.D. degrees from National Taiwan University of Science and Technology, Taipei, Taiwan, in 1980, 1982, and 1989, respectively, all in electrical engineering.

From August 1984 to July 1989, he was an instructor in the Department of Electrical Engineering, National Taiwan University of Science and Technology. He was a visiting scholar in the Wisconsin Electric Machines and Power Electronics Consortium (WEMPEC) at the University of Wisconsin, Madison, from September 1990 to August 1991, and in the Center of Power Electronics Systems (CPES) at Virginia Tech from July 1999 to January 2000. From August 1989 to January 1996, he was an associate professor in the Department of Electrical Engineering, National Taiwan University of Science and Technology, where since February 1996, he has been a professor. His research interests include motor controls, power electronics, and microprocessor-based control systems.

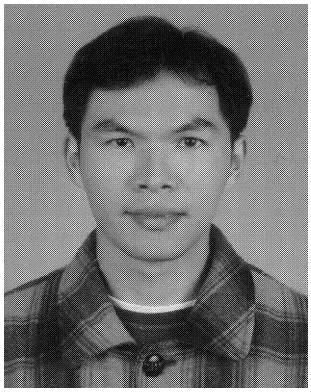

Yung-Ching Lee received the B.S. degree in automatic control engineering from Feng Chia University, Taichung, Taiwan, in 2000 and the M.S. degree in electrical engineering from National Taiwan University of Science and Technology, Taipei, Taiwan, in 2002.

He is now working for Mustek, Hsinchu, Taiwan, where he is involved with the development of the servo control for DVD player applications. His research interests include TV tuner module design, high-performance ac and dc motor drives, and single-chip applications for consumer products.

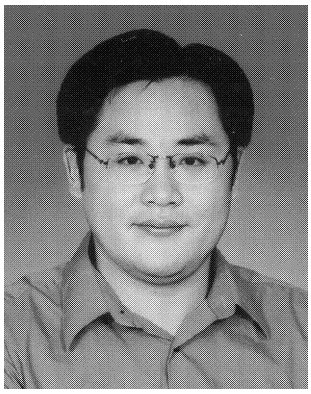

Yih-Hua Chang was born in Taipei, Taiwan, Republic of China, on November 16, 1973. He received the B.S. degree in electronic engineering from Fu Jen University, Taiwan, in 1997 and the M.S. degree in electrical engineering from National Taiwan University of Science and Technology, Taiwan, in 1999, respectively.

Currently, he is a Ph.D. student at National Taiwan University of Science and Technology. His research interests include electric-machine drives and power converter technology.